

# Forward physics with proton tagging at the LHC

**Christophe Royon**

CEA/IRFU/Service de physique des particules, CEA/Saclay, 91191 Gif-sur-Yvette cedex, France

**Abstract.** We present some inclusive and exclusive diffractive processes to be studied at the LHC, namely QCD, quartic anomalous couplings between  $\gamma$  and  $W/Z$  bosons and diffractive Higgs processes.

In this short report, we discuss some potential measurements to be performed using proton tagging detectors at the LHC. We can distinguish two kinds of measurements: the first motivation of these detectors is a better understanding of the structure of the colorless exchanged object, the Pomeron, in a domain of energy unexplored until today and the second motivation is to explore beyond standard model physics such as quartic anomalous couplings between photons and  $W/Z$  bosons and  $\gamma$ . We assume in the following intact protons to be tagged in dedicated detectors located at about 210 m for ATLAS (220 m for CMS) as described at the end of this report.

## 1. Inclusive diffraction measurement at the LHC

In this section, we discuss potential measurements at the LHC that can constrain the Pomeron structure, the colorless object which is exchanged in diffractive interactions. The Pomeron structure in terms of quarks and gluons has been derived from QCD fits at HERA and it is possible to probe this structure and the QCD evolution at the LHC.

### 1.1. Jet production in double Pomeron exchanges processes

The high energy and luminosity at the LHC allow the exploration of a completely new kinematical domain. Tagging both diffractive protons in ATLAS will allow the QCD evolution of the gluon and quark densities in the Pomeron to be probed and the gluon and quark densities to be measured using the dijet and  $\gamma + jet$  cross-section measurements. The different diagrams of the processes that can be studied at the LHC are shown in Fig. 1, namely double pomeron exchange (DPE) production of dijets (left), of  $\gamma$ +jet sensitive respectively to the gluon and quark contents of the Pomeron, and the jet gap jet events (right). As an example, we show in Fig.2, the jet  $p_T$  distribution for  $10 \text{ pb}^{-1}$  for DPE dijet production when the protons are tagged in the ATLAS Forward Physics detectors (AFP). In order to stress the poorly known gluon density at high  $\beta$  (the fraction of the Pomeron momentum carried by the struck parton), we multiply the gluon density by  $(1 - \beta)^\nu$  where  $\nu$  varies between -1 and 1. When  $\nu = -1$  (respectively 1), the gluon density at high  $\beta$  is enhanced (respectively decreased). The ATLAS data will allow constrain of the gluon density further by allowing in particular its measurement at high energy and  $\beta$ . In Fig. 2, the effects of the  $\nu$  variation lead to a difference of factor 40 at high jet  $p_T$  in the jet production cross section.

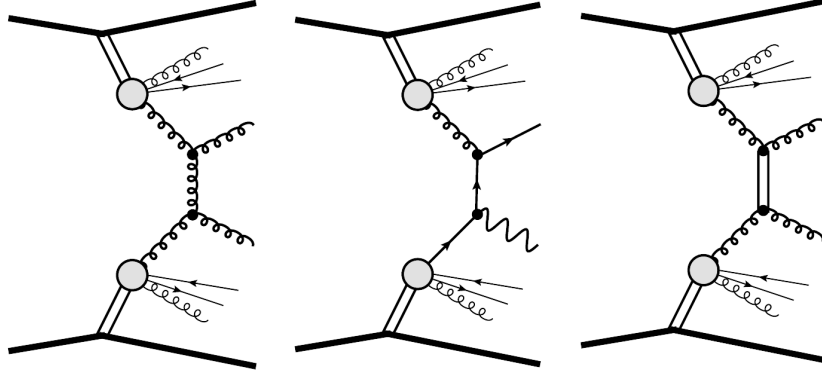


**Figure 1.** Inclusive diffractive diagrams. From left to right: jet production in inclusive double pomeron exchange,  $\gamma$ +jet production in DPE, jet gap jet events

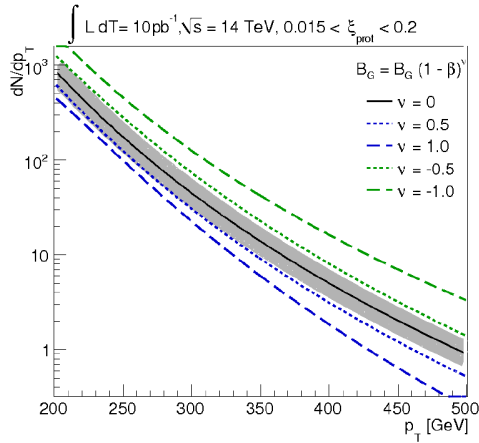


**Figure 2.** Dijet production in DPE events and sensitivity to the gluon density in the Pomeron.

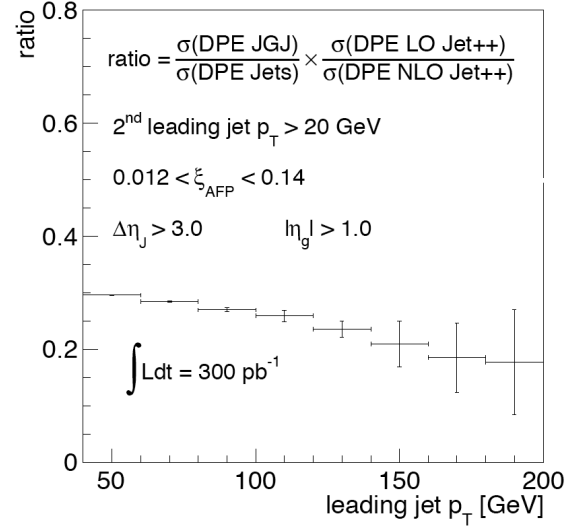


**Figure 3.** Ratio of DPE Jet gap jet events to standard DPE dijet events as a function of the leading jet  $p_T$  [1].

### 1.2. Jet gap jet production in double Pomeron exchanges processes

This process is illustrated in Fig 1, right [1, 2]. Both protons are intact after the interaction and detected in AFP, two jets are measured in the ATLAS central detector and a gap devoid of any energy is present between the two jets. This kind of event is important since it is sensitive to QCD resummation dynamics given by the Balitsky Fadin Kuraev Lipatov [3] (BFKL) evolution equation. This process has never been measured to date and will be one of the best methods to probe these resummation effects, benefitting from the fact that one can perform the measurement for jets separated by a large angle (there is no remnants which ‘pollute’ the event). As an example, the cross section ratio for events with gaps to events with or without gaps as a function of the leading jet  $p_T$  is shown in Fig 3 for  $300 \text{ pb}^{-1}$ .

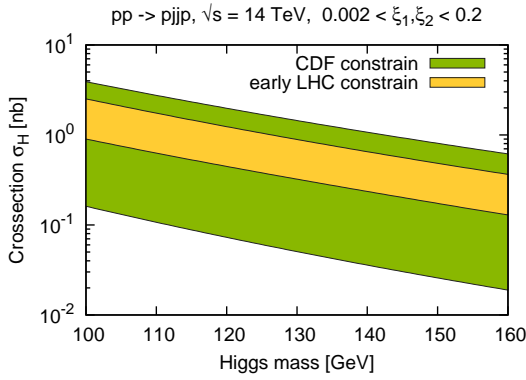


**Figure 4.** Total uncertainty for exclusive Higgs production at the LHC: constraint provided by the CDF measurements and the possible LHC measurement with a luminosity of  $100 \text{ pb}^{-1}$  [7].

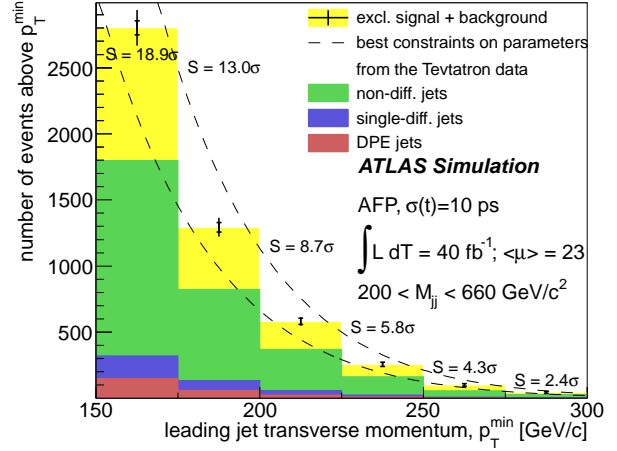


**Figure 5.** Measurement of the exclusive jet production at the LHC in the ATLAS experiment [8].

## 2. Exclusive jet and Higgs boson production at the LHC

The Higgs and jet exclusive production in both Khoze Martin Ryskin [4] (KMR) and CHiDe [5] models have been implemented in the Forward Physics Monte Carlo (FPMC) [6], a generator that has been designed to study forward physics, especially at the LHC. It aims to provide a variety of diffractive processes in one common framework, *i.e.* single diffraction, double pomeron exchange, central exclusive production and two-photon exchange.

Different uncertainties are associated with the models of exclusive diffractive processes. There are three main sources of uncertainties: the gap survival probability which will be measured using the first LHC data (in this study we assume a value of 0.1 at the Tevatron and 0.03 at the LHC), the gluon density, which contains the hard and the soft part (contrary to the hard part, the soft one is not known precisely and originates from a phenomenological parametrisation), and finally the limits of the Sudakov integral which appear in the calculation of exclusive processes, which have not been all fixed by theoretical calculations (apart from the upper limit for the Higgs case) and thus are not known precisely [7].

In order to constrain the uncertainty on the Higgs boson cross section, we study the possible constraints using early LHC measurements of exclusive jets using an integrated luminosity of  $100 \text{ pb}^{-1}$ . In addition to the statistical uncertainties, we consider a conservative 3% jet energy scale uncertainty as the dominant contribution to the systematic error. We obtain the prediction for Higgs boson prediction as shown in Fig. 4 (yellow band).

A possible measurement of exclusive jet cross section (see Fig. 6) at the LHC in the ATLAS experiment is shown in Fig. 5. The results of the measurement is shown as black points for a luminosity of  $40 \text{ fb}^{-1}$  and 23 pile up events, assuming the protons to be detected in the ATLAS Forward Physics detectors [8]. The expected contributions from background (non-diffractive, single diffractive with pile up and double pomeron exchange events) are shown as well as the exclusive jet one in yellow. The statistical significance of the measurement is up to  $19\sigma$ .

## 3. Exclusive $WW$ and $ZZ$ production

In the Standard Model (SM) of particle physics, the couplings of fermions and gauge bosons are constrained by the gauge symmetries of the Lagrangian. The measurement of  $W$  and  $Z$

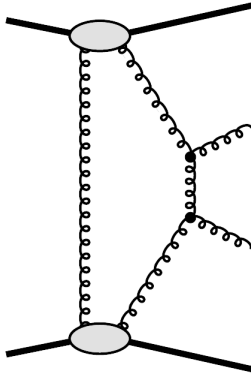


**Figure 6.** Exclusive jet production.

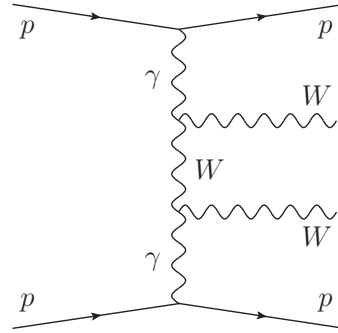


**Figure 7.** Diagram showing the two-photon production of  $W$  pairs.

boson pair productions via the exchange of two photons allows to provide directly stringent tests of one of the most important and least understood mechanism in particle physics, namely the electroweak symmetry breaking.

### 3.1. Photon exchange processes in the SM

The process that we intend to study is the  $W$  pair production shown in Fig. 7 induced by the exchange of two photons [9]. It is a pure QED process in which the decay products of the  $W$  bosons are measured in the central detector and the scattered protons leave intact in the beam pipe at very small angles

After simple cuts to select exclusive  $W$  pairs decaying into leptons, such as a cut on the proton momentum loss of the proton ( $0.0015 < \xi < 0.15$ ) — we assume the protons to be tagged in the ATLAS Forward Physics detectors [8] — on the transverse momentum of the leading and second leading leptons at 25 and 10 GeV respectively, on  $\cancel{E}_T > 20$  GeV,  $\Delta\phi > 2.7$  between leading leptons, and  $160 < W < 500$  GeV, the diffractive mass reconstructed using the forward detectors, the background is found to be less than 1.7 event for  $30 \text{ fb}^{-1}$  for a SM signal of 51 events.

### 3.2. Quartic anomalous couplings

The parameterization of the quartic couplings based on [10] is adopted. The cuts to select quartic anomalous gauge coupling  $WW$  events are similar as the ones we mentioned in the previous section, namely  $0.0015 < \xi < 0.15$  for the tagged protons,  $\cancel{E}_T > 20$  GeV,  $\Delta\phi < 3.13$  between the two leptons. In addition, a cut on the  $p_T$  of the leading lepton  $p_T > 160$  GeV and on the diffractive mass  $W > 800$  GeV are requested since anomalous coupling events appear at high mass. Fig 8 displays the  $p_T$  distribution of the leading lepton for signal and the different considered backgrounds. After these requirements, we expect about 0.7 background events for an expected signal of 17 events if the anomalous coupling is about four orders of magnitude lower than the present LEP limit ( $|a_0^W/\Lambda^2| = 5.4 \cdot 10^{-6}$ ) for a luminosity of  $30 \text{ fb}^{-1}$ . The strategy to select anomalous coupling  $ZZ$  events is analogous and the presence of three leptons or two like sign leptons are requested. Table 1 gives the reach on anomalous couplings at the LHC for luminosities of 30 and  $200 \text{ fb}^{-1}$  compared to the present OPAL limits [11]. We note that we can gain almost four orders of magnitude in the sensitivity to anomalous quartic gauge couplings compared to LEP experiments, and it is possible to reach the values expected in extra-dimension models. The tagging of the protons using the ATLAS Forward Physics detectors is the only method at present to test so small values of quartic anomalous couplings.

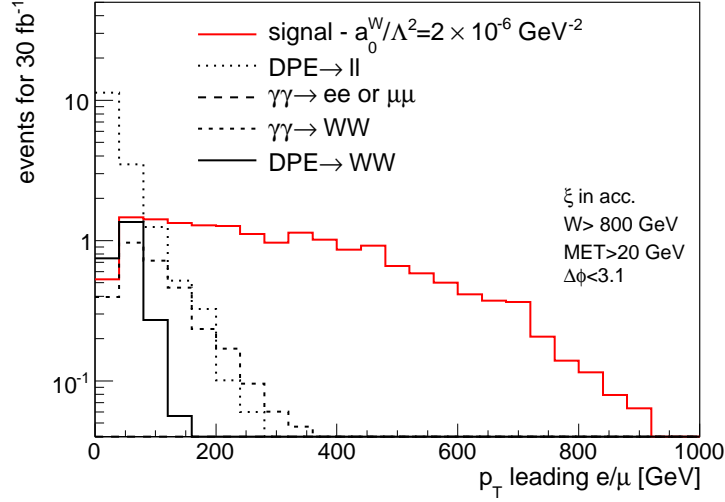


**Figure 8.** Distribution of the transverse momentum of the leading lepton for signal and background after the cut on  $W$ ,  $\cancel{E}_T$ , and  $\Delta\phi$  between the two leptons [9].

Couplings	OPAL limits [GeV <sup>-2</sup> ]	Sensitivity @ $\mathcal{L} = 30$ (200) fb <sup>-1</sup>	
		5 $\sigma$	95% CL
$a_0^W/\Lambda^2$	[-0.020, 0.020]	$5.4 \cdot 10^{-6}$ ( $2.7 \cdot 10^{-6}$ )	$2.6 \cdot 10^{-6}$ ( $1.4 \cdot 10^{-6}$ )
$a_C^W/\Lambda^2$	[-0.052, 0.037]	$2.0 \cdot 10^{-5}$ ( $9.6 \cdot 10^{-6}$ )	$9.4 \cdot 10^{-6}$ ( $5.2 \cdot 10^{-6}$ )
$a_0^Z/\Lambda^2$	[-0.007, 0.023]	$1.4 \cdot 10^{-5}$ ( $5.5 \cdot 10^{-6}$ )	$6.4 \cdot 10^{-6}$ ( $2.5 \cdot 10^{-6}$ )
$a_C^Z/\Lambda^2$	[-0.029, 0.029]	$5.2 \cdot 10^{-5}$ ( $2.0 \cdot 10^{-5}$ )	$2.4 \cdot 10^{-5}$ ( $9.2 \cdot 10^{-6}$ )

**Table 1.** Reach on anomalous couplings obtained in  $\gamma$  induced processes after tagging the protons in AFP compared to the present OPAL limits. The 5 $\sigma$  discovery and 95% C.L. limits are given for a luminosity of 30 and 200 fb<sup>-1</sup> [9]

As mentioned already, in order to achieve this experimental program, a proposal to add forward proton detectors located at 210 m (respectively 240) and 420 m from the interaction point was submitted to the ATLAS (respectively CMS) collaborations. Both detectors allow a good acceptance in mass between 110 GeV and 1.4 TeV. By 2014, only the 210 m detectors are foreseen. They are sensitive to high diffractive masses and will allow to fulfill the program to look for anomalous couplings extra-dimension models with an unprecedented precision if these projects are approved by the ATLAS and CMS collaborations.

The search for quartic anomalous couplings between  $\gamma$  and  $W$  bosons was performed again after a full simulation of the ATLAS detector including pile up [8]. Integrated luminosities of 40 and 300 fb<sup>-1</sup> with, respectively, 23 or 46 average pile-up events per beam crossing have been considered. The  $W$  pair is assumed to decay leptonically. The full list of background processes used for the ATLAS measurement of Standard Model  $WW$  cross-section was simulated, namely  $t\bar{t}$ ,  $WW$ ,  $WZ$ ,  $ZZ$ ,  $W$ +jets, Drell-Yan and single top events. In addition, the

additional diffractive backgrounds mentioned in the previous paragraph were also simulated. The requirement of the presence of at least one proton on each side of AFP within a time window of 10 ps allows us to reduce the background by a factor of about 200 (50) for  $\mu = 23$  (46). The  $p_T$  of the leading lepton originating from the leptonic decay of the  $W$  bosons is required to be  $p_T > 150$  GeV, and that of the next-to-leading lepton  $p_T > 20$  GeV. Additional requirement of the dilepton mass to be above 300 GeV allows us to remove most of the  $Z$  and  $WW$  events. Since only leptonic decays of the  $W$  bosons are considered, we require in addition less than 3 tracks associated to the primary vertex, which allows us to reject a large fraction of the non-diffractive backgrounds (e.g.  $t\bar{t}$ , diboson productions,  $W$ +jet, etc.) since they show much higher track multiplicities. Remaining Drell-Yan and QED backgrounds are suppressed by requiring the difference in azimuthal angle between the two leptons  $\Delta\phi < 3.1$ . After these requirements, a similar sensitivity with respect to fast simulation without pile up was obtained.

Of special interest will be also the search for anomalous quartic  $\gamma\gamma\gamma\gamma$  anomalous couplings which is now being implemented in the FPMC generator. Let us notice that there is no present existing limit on such coupling and the sensitivity using the forward proton detectors is expected to be similar as the one for  $\gamma\gamma WW$  or  $\gamma\gamma ZZ$  anomalous couplings. If discovered at the LHC,  $\gamma\gamma\gamma\gamma$  quartic anomalous couplings might be related to the existence of extra-dimensions in the universe, which might lead to a reinterpretation of some experiments in atomic physics. As an example, the Aspect photon correlation experiments [12] might be interpreted via the existence of extra-dimensions. Photons could communicate through extra-dimensions and the deterministic interpretation of Einstein for these experiments might be true if such anomalous couplings exist. From the point of view of atomic physics, the results of the Aspect experiments would depend on the distance of the two photon sources.

#### 4. Forward Proton Detectors in ATLAS and CMS

In this section, we describe the proposal to install the ATLAS Forward Proton (AFP) detector in order to detect intact protons at 206 and 214 meters on both side of the ATLAS experiment [8] (similar detectors will be installed around CMS by TOTEM/CMS). This one arm will consist of two sections (AFP1 and AFP2) contained in a special design of beam pipe (or in more traditional roman pots). In the first section (AFP1), in one pocket of the beam pipe, a tracking station composed by 6 layers of Silicon detectors will be deployed. The second station AFP2 will contain another tracking station similar to the one already described and a timing detector. The aim of this setup, mirrored by an identical arm placed on the opposite side of the ATLAS interaction point, will be to tag the protons emerging intact from the  $pp$  interactions so allowing ATLAS to exploit the program of diffractive and photoproduction processes described in the previous sections.

##### 4.1. Movable beam pipes

The idea of movable Hamburg beam pipes is quite simple [13]: a larger section of the LHC beam pipe than the usual one can move close to the beam using bellows so that the detectors located at its edge (called pocket) can move close to the beam by about 2.5 cm when the beam is stable (during injection, the detectors are in parking position). In its design, the predominant aspect is the minimization of the thickness of the portions called floor and window (see Fig. 9). Minimizing the depth of the floor ensures that the detector can go as close to the beam as possible allowing us to detect protons scattered at very small angles, while minimizing the depth of the thin window is important to keep the protons intact and to reduce the impact of multiple interactions. Two configurations exist for the movable beam pipes: the first one at 206 m from the ATLAS interaction point hosts a Si detector (floor length of about 100 mm) and the second one (floor length of about 400 mm) the timing and the Si detectors.

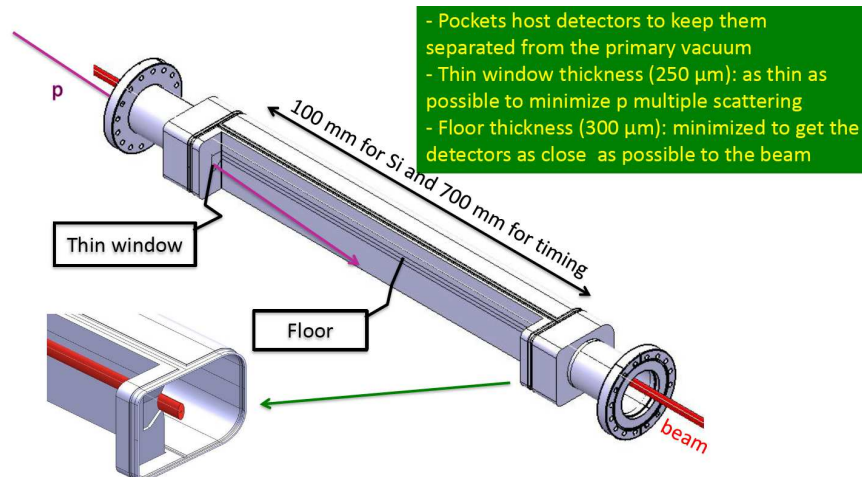


**Figure 9.** Scheme of the movable beam pipe.

#### 4.2. 3D Silicon detectors

The purpose of the tracker system is to measure points along the trajectory of beam protons that are deflected at small angles as a result of collisions. The tracker when combined with the LHC dipole and quadrupole magnets, forms a powerful momentum spectrometer. Silicon tracker stations will be installed in Hamburg beam pipes (HBP) at  $\pm 206$  and  $\pm 214$  m from the ATLAS.

The key requirements for the silicon tracking system at 220 m are:

- Spatial resolution of  $\sim 10$  (30)  $\mu\text{m}$  per detector station in  $x$  ( $y$ )
- Angular resolution for a pair of detectors of about  $1 \mu\text{rad}$
- High efficiency over the area of  $20 \text{ mm} \times 20 \text{ mm}$  corresponding to the distribution of diffracted protons
- Minimal dead space at the edge of the sensors allowing us to measure the scattered protons at low angles
- Sufficient radiation hardness in order to sustain the radiation at high luminosity
- Capable of robust and reliable operation at high LHC luminosity

The basic building unit of the AFP detection system is a module consisting of an assembly of a sensor array, on-sensor read-out chip(s), electrical services, data acquisition and detector control system. The module will be mounted on the mechanical support with embedded cooling and other necessary services. The sensors are double sided 3D  $50 \times 250$  micron pixel detectors with slim-edge dicing built by FBK and CNM companies. The sensor efficiency has been measured to be close to 100% over the full size in beam tests. A possible upgrade of this device will be to use 3D edgeless Silicon detectors built in a collaboration between SLAC, Manchester, Oslo, Bergen... A new front-end chip FE-I4 has been developed for the Si detector by the Insertable B Layer (IBL) collaboration in ATLAS. The FE-I4 integrated circuit contains readout circuitry for 26 880 hybrid pixels arranged in 80 columns on  $250 \mu\text{m}$  pitch by 336 rows on  $50 \mu\text{m}$  pitch, and covers an area of about  $19 \text{ mm} \times 20 \text{ mm}$ . It is designed in a 130 nm feature size bulk CMOS process. Sensors must be DC coupled to FE-I4 with negative charge collection. The FE-I4 is very well suited to the AFP requirements: the granularity of cells provides a sufficient spatial resolution, the chip is radiation hard enough (up to a dose of 3 MGy), and the size of the chip is sufficiently large that one module can be served by just one chip.

The dimensions of the individual cells in the FE-I4 chip are  $50\text{ }\mu\text{m} \times 250\text{ }\mu\text{m}$  in the  $x$  and  $y$  directions, respectively. Therefore to achieve the required position resolution in the  $x$ -direction of  $\sim 10\text{ }\mu\text{m}$ , six layers with sensors are required (this gives  $50/\sqrt{12}/\sqrt{5} \sim 7\text{ }\mu\text{m}$  in  $x$  and roughly 5 times worse in  $y$ ). Offsetting planes alternately to the left and right by one half pixel will give a further reduction in resolution of at least 30%. The AFP sensors are expected to be exposed to a dose of 30 kGy per year at the full LHC luminosity of  $10^{34}\text{cm}^{-2}\text{s}^{-1}$ .

#### 4.3. Timing detectors

A fast timing system that can precisely measure the time difference between outgoing scattered protons is a key component of the AFP detector. The time difference is equivalent to a constraint on the event vertex, thus the AFP timing detector can be used to reject overlap background by establishing that the two scattered protons did not originate from the same vertex as the central system. The final timing system should have the following characteristics [15]:

- 10 ps or better resolution (which leads to a factor 40 rejection on pile up background)
- Efficiency close to 100% over the full detector coverage
- High rate capability (there is a bunch crossing every 25 ns at the nominal LHC)
- Enough segmentation for multi-proton timing
- Level trigger capability

Figure 10 shows a schematic overview of the first proposed timing system, consisting of a quartz-based Cerenkov detector coupled to a microchannel plate photomultiplier tube (MCP-PMT), followed by the electronic elements that amplify, measure, and record the time of the event along with a stabilized reference clock signal. The QUARTIC detector consists of an array of  $8 \times 4$  fused silica bars ranging in length from about 8 to 12 cm and oriented at the average Cerenkov angle. A proton that is sufficiently deflected from the beam axis will pass through a row of eight bars emitting Cerenkov photons providing an overall time resolution that is approximately  $\sqrt{8}$  times smaller than the single bar resolution of about 30 ps, thus approaching the 10 ps resolution goal. Prototype tests have generally been performed on one row (8 channels) of  $5\text{ mm} \times 5\text{ mm}$  pixels, while the initial detector is foreseen to have four rows to obtain full acceptance out to 20 mm from the beam. The beam tests lead to a time resolution per bar of the order of 34 ps. The different components of the timing resolution are given in Fig. 11. The upgraded design of the timing detector has equal rate pixels, and we plan to reduce the width of detector bins close to the beam, where the proton density is highest.

At higher luminosity of the LHC (phase I starting in 2019), higher pixelisation of the timing detector will be required. For this sake, a R&D phase concerning timing detector developments based on Silicon photomultipliers (SiPMs), avalanche photodiodes (APDs), quartz fibers, diamonds has been started in Saclay. In parallel, a new timing readout chip has been developed. It uses waveform sampling methods which give the best possible timing resolution. The aim of this chip called SAMPIC [16] is to obtain sub 10 ps timing resolution, 1GHz input bandwidth, no dead time at the LHC, and data taking at 2 Gigasamples per second. The cost per channel is estimated to be of the order for \$10 which is a considerable improvement to the present cost of a few \$1000 per channel, allowing us to use this chip in medical applications such as PET imaging detectors. The holy grail of imaging 10 picosecond PET detector seems now to be feasible: with a resolution better than 20 ps, image reconstruction is no longer necessary and real-time image formation becomes possible.

## 5. References

- [1] C. Marquet, C. Royon, M. Trzebinski, R. Zlebcik, arXiv:1212.2059, accepted by Phys. Rev. D; O. Kepka, C. Marquet, C. Royon, Phys. Rev. D **83** (2011) 034036.



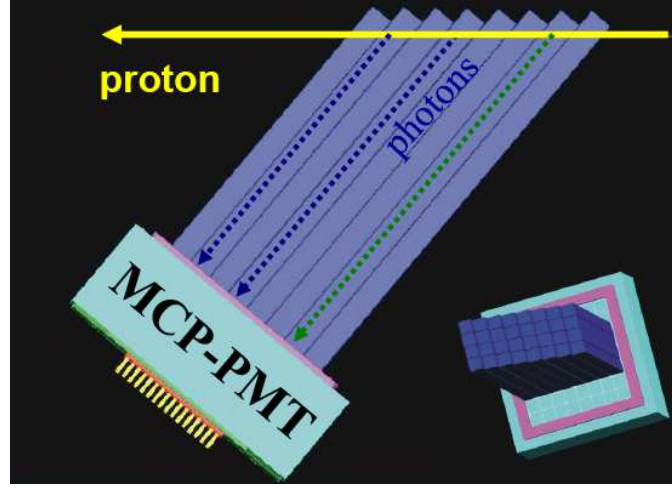


**Figure 10.** A schematic diagram of the QUARTIC fast timing detector.

Component	$\delta t(\text{ps})$ Current	$\delta t(\text{ps})$ Projected (8 ch + cable)	Improve ment	$\delta t(\text{ps})$ Phase 0 (8 channels)
Radiator (fused silica bar) ~10 pe's	22	22	Optimize radiator	17
MCP-PMT (64 channel 25 um Planacon)	20	20	10 um tube	15
CFD	5	5	-	5
HPTDC	16	16	-	15
Reference Clock	-	3	-	3
Total/bar	34	34		28
Cable		15%	retune CFD	5%
Total/ detector	14	14	-	10

**Figure 11.** Different components of the timing detector resolution [15].

- [2] C. Marquet, C. Royon, Phys. Rev. D **79** (2009) 034028; O. Kepka, C. Royon, C. Marquet, R. Peschanski, Eur. Phys. J. C **55** (2008) 259-272; Phys. Lett. B **655** (2007) 236-240; H. Navelet, R. Peschanski, C. Royon, S. Wallon, Phys. Lett. B **385** (1996) 357; H. Navelet, R. Peschanski, C. Royon, Phys. Lett. B **366** (1996) 329.
- [3] V. S. Fadin, E. A. Kuraev, L. N. Lipatov, Phys. Lett. B **60** (1975) 50; I. I. Balitsky, L. N. Lipatov, Sov.J.Nucl.Phys. **28** (1978) 822;
- [4] V. A. Khoze, A. D. Martin and M. G. Ryskin, Eur. Phys. J. C **23** (2002) 311.
- [5] J. R. Cudell, A. Dechambre, O. F. Hernandez and I. P. Ivanov, Eur. Phys. J. C **61** (2009) 369.
- [6] M. Boonekamp, A. Dechambre, V. Juranek, O. Kepka, M. Rangel, C. Royon, R. Staszewski, e-Print: arXiv:1102.2531; M. Boonekamp, V. Juranek, O. Kepka, C. Royon "Forward Physics Monte Carlo", "Proceedings of the workshop: HERA and the LHC workshop series on the implications of HERA for LHC physics," arXiv:0903.3861 [hep-ph].
- [7] A. Dechambre, O. Kepka, C. Royon, R. Staszewski, Phys. Rev. D **83** (2011) 054013. 14; T. Coughlin, J. Forshaw, PoS DIS2010 (2010) 064.
- [8] ATLAS Coll., CERN-LHCC-2011-012.
- [9] E. Chapon, O. Kepka, C. Royon, Phys. Rev. D **81** (2010) 074003; O. Kepka and C. Royon, Phys. Rev. D **78** (2008) 073005; J. de Favereau et al., preprint arXiv:0908.2020.
- [10] G. Belanger and F. Boudjema, Phys. Lett. B **288** (1992) 201.
- [11] G. Abbiendi *et al.* [OPAL Collaboration], Phys. Rev. D **70** (2004) 032005 [arXiv:hep-ex/0402021].
- [12] A. Aspect, P. Grangier, G. Roger, Phys. Rev. Lett., Vol. 49, no 2 (1982) 91-94; A. Aspect, J. Dalibard, G. Roger, Phys. Rev. Lett., Vol. 49, Iss. 25 (1982) 1804.

- [13] K. Piotrkowski, U. Schneekloth, Proc. of the ZEUS Collaboration meeting, March 1994, DESY, Hamburg.
- [14] ATLAS IBL Coll., CERN-LHCC-2010-013, ATLAS-TDR-019 5/09/2010.
- [15] A. Brandt, Microchannel Plate PMT Lifetime and Performance, DIRC2011: Workshop on Fast Cerenkov detectors, Giessen, Germany, April 4-6, 2011.
- [16] E. Delagnes, D. Breton, F. Lugiez, R. Rahmanifard, Nucl. Science IEEE Transactions, Volume 54, Issue 5, Part 2, Oct 2007, 1735; E. Delagnes, patent WO 2008/050177, EP2076963.